Proceedings of Ninth World Conference on Earthquake Engineering
August 2-9, 1988, Tokyo-Kyoto, JAPAN (Vol.IV)

6-3-9

STATIC AND DYNAMIC ANALYSIS OF FULL-SCALE CONCENTRICALLY K-BRACED STEEL BUILDING

Mitsumasa MIDORIKAWA[1], Isao NISHIYAMA[2], and Hiroyuki YAMANOUCHI[3]

1 Senior Research Struct. Engr., Building Research Inst., Ministry of Construction, 1 Tatehara, Tsukuba, Ibaraki 305, Japan.
2 Senior Research Struct. Engr., Building Research Inst., MOC.
3 Head of Struct. Dynamics Div., Building Research Inst., MOC.

SUMMARY

Presented is the analytical estimation of full-scale seismic tests on a K-braced steel building. A computer program for the inelastic frame analysis is used to calculate the static and dynamic responses of the test building. From a comparison of the analytical and experimental results, the overall and local behavior of the test building subjected to simulated earthquakes can be reasonably well represented by using the implemented model and analytical method.

INTRODUCTION

As part of the U.S./Japan Cooperative Research Program, a full-scale six-story steel building was designed, constructed and tested at the Building Research Institute (BRI). This paper is the analytical estimation on a series of seismic tests on the concentrically K-braced steel building (Ref. 1). The test building consisted of three frames parallel to the loading direction, and three frames perpendicular to the loading direction. In the loading direction, the two exterior frames were of ductile moment-resisting type. The central longitudinal frame was braced with concentric K-bracing of square tubes. In the transverse direction, the two exterior frames were diagonally braced in all bays. Details of the test building are described in Ref. 1. The seismic tests were run as a six-degree-of-freedom pseudo-dynamic (PSD) system. The earthquake record chosen as input excitation was the NS component of strong-motion accelerogram recorded at Tohoku Uni., Miyagi-Ken, July 12, 1978, as shown in Fig. 1. The peak acceleration was scaled to an appropriate value corresponding to three major seismic tests: "Elastic PSD Test" with 0.65 m/sec^2 (6.6 %g) peak value, "Inelastic PSD Moderate Test" with 2.50 m/sec^2 (26 %g) peak value, and "Inelastic PSD Final Test" with 5.00 m/sec^2 (51 %g) peak value.

ANALYTICAL MODELING AND METHODS

The modified version of the nonlinear dynamic analysis computer program DRAIN-2D (Ref. 2) is used to predict the responses of the building. The mathematical idealization of the building is illustrated in Fig. 2. The adopted element types and their characteristics are listed in Table 1. The main assumptions to model the building are as follows: (1) With regard to beam-column, beam and end moment-buckling elements, flexural and axial deformations are taken into account. Shear deformations are also considered in beam-column elements. (2) Center-to-center dimensions in member length are used in principle. (3) Yield

moments are represented by full-plastic moments. (4) Yield moments of members at the nodal point are extrapolated by assuming the double curvature moment distribution along member length and the plastic hinges at member ends. (5) Yielding of members follows kinematic hardening schemes. (6) The strain hardening stiffness in principle is set at 5% of elastic one. (7) The yield stress of steel and the compressive strength of concrete are the coupon test and the cylinder test values, respectively. (8) An in-plane flexible floor diaphragm and an axial deformation of a composite girder are assumed. (9) Restraint on a column axial deformation by the diagonal braces and the girders in the transverse direction is considered. (10) In beam-column elements, rigid and infinitely strong connecting links are assumed between the nodal points and the column ends. (11) All column bases are fixed. (12) Reactive weights are assumed to be lumped at each nodal point.

The degrading hysteresis model for end moment-buckling elements is developed to simulate the post-buckling and hysteretic behavior of bracing members as illustrated in Fig. 3 (Ref. 3). This model is developed by modifying the hysteresis rule (Ref. 4) in the post-buckling range. The initial buckling strength (Pyn) is calculated using the following formula (Ref. 5):

$$Pyn = Pyp\{1-0.545(\lambda-0.3)\} \quad (1)$$

where $$\lambda = (1/\pi)\sqrt{fy/E}\,(KL/r) \quad (2)$$

; Pyp = axial yield strength; fy = yield stress; E = Young's modulus; K = effective length factor; L = face-to-face length; and r = radius of gyration. The buckling load reduction factor, Pync/Pyn, is estimated to be 18/(KL/r) (Ref. 4). The effective length factor, K, is assumed to be 0.7. It is assumed that the viscous damping results from a combination of mass-dependent and initial stiffness-dependent effects. The critical damping ratios of 0.5% are introduced to the first two modes, which are compatible with the vibration test results.

RESULTS AND DISCUSSIONS OF STATIC ANALYSIS

The inelastic response of the building under monotonic loading is obtained from the static frame analysis with use of the modified version of DRAIN-2D program. The distribution of the seismic forces along the height of the building is in accordance with the Japanese design code. Fig. 4 shows the story shear vs. interstory displacement relations. The base shears obtained from the analysis are 324 tonf at the first story brace buckling and 327 tonf at the collapse mechanism, which are 2% and 1% lower than the measured maximum base shear of 331 tonf, respectively. Fig. 5 shows the analytical collapse mechanism. The observed damage pattern after Final Test is shown in Fig. 6. Many joint panel zones and member ends suffered damage mainly at the lower three stories. The analytical collapse machanism does not contradict with the experimental damage pattern.

RESULTS AND DISCUSSIONS OF DYNAMIC ANALYSIS

The maximum responses obtained from the analysis are listed in Table 2. The envelopes of the maximum responses of the building are shown in Fig. 7. The comparison of the analytical results with the experimental ones is shown in the figures of the following sections, where the analytical results are indicated with dotted/dashed lines and the experimental ones with solid lines.

Analysis for Elastic PSD Test The horizontal roof displacement time histories are shown in Fig. 8(a). The periods of the response agree with each other excellently. The analytical response, however, shows a tendency to be larger than the experimental one. The discrepancy of the maximum floor displacements is 13 to 16% between the analysis and the test as in Table 2 and Fig. 7(a). This is mainly due to the effects of the testing control algorithm adopted in the PSD test system and very slight hysteretic damping observed in Elastic Test. The former effect reduces the floor displacement by about 4% and the latter effect by about 8%.

Analysis for Inelastic PSD Moderate Test The horizontal roof displacement time history from the analysis matches very good with the test result up to about 15 sec. as shown in Fig. 8(b). The analysis cannot follow the test during the last few cycles, because of the yielding and the failure of the shear panel zone of the girder connection at the second floor between the first story K-braces, which was repaired after Moderate Test. The maximum floor displacements from the analysis are smaller by 5 to 10% than those from the test as in Table 2 and Fig. 7(a). The difference of the maximum interstory displacements between the analysis and the test is within 6% above the second story and 10% at the first story.

Analysis for Inelastic PSD Final Test The parameters of the brace hysteresis rule are set for two cases: the brace models 1 and 2. In the brace model 1, the initial buckling strength (Pyn) is calculated by the design formula, and the parameters of the hysteresis rule follow the proposal by Ref. 4. In the brace model 2, they are fitted to the measured ones.

The horizontal roof displacement time history from the brace model 2 in Fig. 8(d) agrees to the experimental one much better than that from the brace model 1 in Fig. 8(c). The floor displacement response especially after the maximum response in the brace model 2 is more compatible with the experimental one than that in the brace model 1. As in Table 2 and Fig. 7(a), the maximum floor displacements at the upper three floors from the brace model 2 are only a little bit larger within the difference of 7% than the experimental ones. The maximum floor displacements at the lower three floors from the brace model 2 are remarkably improved. The difference between the analysis and the test is reduced to as much as 12 and 5% at the second and third floors, respectively. The story shear vs. interstory displacement relations at the lower two stories are shown in Fig. 9. The distribution of the maximum interstory drifts along the height of the building as in Table 2 and Fig. 7(b) and the envelopes of the hysteresis curves from the brace model 2 as in Fig. 9(b) are more consistent with the experimental results than those from the brace model 1. In the brace model 2, the maximum interstory drift ratios of the analysis to the test are 0.88 to 1.21.

Severe brace buckling was developed at the second and third stories during Final Test. Local tear initiation at the corners of the tubular braces followed the maximum response of the test structure. The axial force vs. axial deformation relations of the north brace at the third story are shown in Fig. 10. The calculated initial buckling strength of the brace is slightly different from the measured one. The envelopes of the brace hysteresis curves are apparently different between the brace model 1 and the test. This implies the limitation of the hysteresis rule of the braces adopted in the brace model 1, which is proposed on the basis of the experimental behavior of braces before the formation of local buckling and so cannot follow the local failure of the braces such as local buckling, kinks and local tears occured during Final Test. The damage pattern of the building obtained from the brace models 1 and 2 are shown in Fig. 11. Although there is some discrepancies between the analysis and the test, the analytical damage pattern from the brace model 2 is more consistent with the experimental one in Fig. 6 than that from the brace model 1.

CONCLUSIONS

1. The maximum base shears and the collapse mechanism obtained from the static analysis are consistent with the experimental results.
2. The analytical response for Elastic PSD Test shows that the vibrational period of the building agrees excellently with the experimental one. The discrepancy of the maximum horizontal floor displacements is 13 to 16% between the analysis and the test. This is mainly attributed to the effects of the testing control algorithm and very slight hysteretic damping in the test.
3. The analytical results for Inelastic PSD Moderate Test match quite well with

the experimental results except for the last few cycles. The difference about the overall response between the analysis and the test is within 10% at most.
4. In the analysis for Inelastic PSD Final Test, the parameters of the brace hysteresis rule are set for two cases. The analytical results from the brace model 2 are much more consistent with the experimental ones than those from the brace model 1, with respect to not only the overall response but also the damage distribution. The difference about the overall response envelopes between the brace model 2 and the test is within 12% in the horizontal floor displacements, and is within 21% in the interstory drifts. In comparison with the analytical results between the two brace models, the overall hysteresis behavior and the damage distribution along the height of the building are affected very much by the difference of the hysteresis characteristics of each bracing member, such as the scattering of the buckling strength and the change of the envelope of the hysteresis curve caused by the local failure.

ACKNOWLEDGEMENTS

This research was funded by the Japanese Ministry of Construction and the U.S. National Science Foundation. The research collaboration was organized with the Building Research Institute, the Kozai Club and the Building Contractors Society in the Japanese side. The authors gratefully acknowledge this support.

REFERENCES

1. Yamanouchi, H., Nishiyama,I., and Midorikawa, M., "Inelastic Behavior of Full-Scale Concentrically K-Braced Steel Building", Proc. 9th WCEE, 1988.
2. Kanaan, A. E., and Powell, G. H., "General Purpose Computer Program for Inelastic Dynamic Response of Plane Structures", Report UCB/EERC-73/6, 1973.
3. Kato, B., and Akiyama, H., "Restoring Force Characteristics of Steel Frames Equipped with Diagonal Bracings", Trans. AIJ, 260, 1977. (in Japanese)
4. Jain, A. K., and Goel, S. C., "Hysteresis Models for Steel Members Subjected to Cyclic Buckling or Cyclic End Moments and Buckling", Rep. UMEE 78R6, 1978.
5. AIJ, "Recommendations for Plastic Design in Steel Structures", the Architectural Institute of Japan, 1975. (in Japanese)

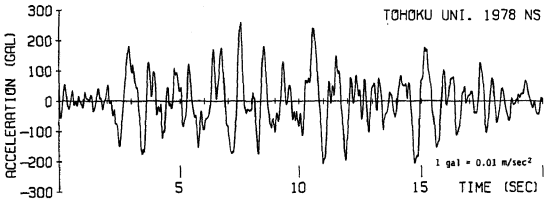

Fig.1 Input Acceleration Record

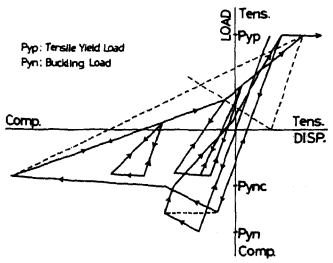

Fig.3 Brace Hysteresis Model

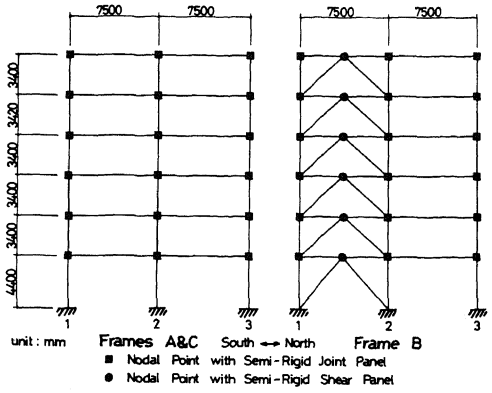

Fig.2 Analytical Model of Building

Table 1 Element Types and Characteristics

Member	Element Type	Force-Disp. Relationship	Yield Interaction Surface	
			Type	Yield Strength Formula
Column	Beam-colum	Bi-linear (end moment-rot.)	II-A[a]	AIJ Recommendations for Plastic Design (1975)[b]
Girder	Beam	Bi-linear (end moment-rot.)	I-A[c]	AIJ Design Recomm. for Composite Constr. (1985)
Joint Panel	Semi-rigid Connection	Bi-linear (moment-rot.)	I-B[d]	AIJ Design Standard for Steel Structures (1970)
Brace	End Moment -buckling	Degrading (axial force-def.)	II-A[a]	AIJ Recommendations for Plastic Design (1975)[b]
Shear Panel	Semi-rigid Connection	Tri-linear (shear force-def.)	I-C[e]	AIJ Design Standard for Steel Structures (1970)

[a] An axial force-bending moment interaction surface is a function of
[b] bi-linear in every quarter of the interaction space.
[c] A compression strength is determined by a buckling strength.
[d] Yielding is affected by bending moment only.
[e] Yielding is affected by moment only.
Yielding is affected by shear force only.

Table 2 Maximum Responses

Analysis	Floor (Story)	Floor Disp.[a]		Story Disp.[a]		Story Shear[a]	
		Disp. (cm)	Ratio[b]	Disp. (cm)	Ratio[b]	Shear (tonf)	Ratio[b]
Elastic PSD Test	R (6)	-3.253	1.13	-0.408	0.92	25.9	0.88
	6 (5)	-2.847	1.16	-0.588	1.11	-52.9	1.09
	5 (4)	-2.266	1.16	-0.590	1.18	-74.2	1.14
	4 (3)	-1.680	1.15	-0.597	1.15	-92.4	1.14
	3 (2)	-1.083	1.15	-0.580	1.16	-106.8	1.14
	2 (1)	-0.503	1.13	-0.503	1.13	-117.0	1.13
Inelastic PSD Moderate Test	R (6)	8.211	0.96	-1.046	1.00	-67.7	1.05
	6 (5)	7.513	0.96	-1.407	1.00	-116.4	0.99
	5 (4)	6.421	0.95	-1.298	0.94	156.5	0.99
	4 (3)	5.233	0.95	1.480	0.95	205.3	1.01
	3 (2)	3.792	0.95	1.930	1.03	254.9	1.06
	2 (1)	1.901	0.90	1.901	0.90	277.4	1.04
Inelastic PSD Final Test (Brace Model 1)	R (6)	-23.250	1.06	-1.198	1.00	81.6	1.10
	6 (5)	-22.074	1.05	-3.949	1.85	-147.3	1.08
	5 (4)	-18.802	1.00	-4.907	1.63	-193.8	1.03
	4 (3)	-14.224	0.90	-6.196	1.12	-255.5	1.12
	3 (2)	-8.055	0.76	-5.211	0.87	290.4	1.11
	2 (1)	-2.978	0.64	-2.978	0.64	325.1	0.98
Inelastic PSD Final Test (Brace Model 2)	R (6)	-23.576	1.07	1.279	1.07	85.9	1.16
	6 (5)	-22.461	1.07	-2.559	1.20	158.8	1.16
	5 (4)	-20.008	1.06	-3.635	1.21	191.1	1.02
	4 (3)	-16.470	1.04	-6.378	1.15	-249.7	1.09
	3 (2)	-10.133	0.95	-6.185	1.03	298.6	1.15
	2 (1)	-4.075	0.88	-4.075	0.88	345.1	1.04

[a] Displacement and force to the south are positive.
[b] Ratios of analysis to test results.

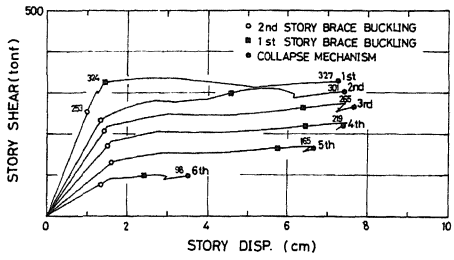

Fig.4 Story Shear vs. Story Drift Relationships

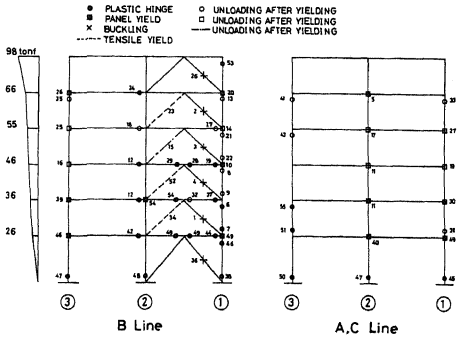

Fig.5 Collapse Mechanism : Static Analysis

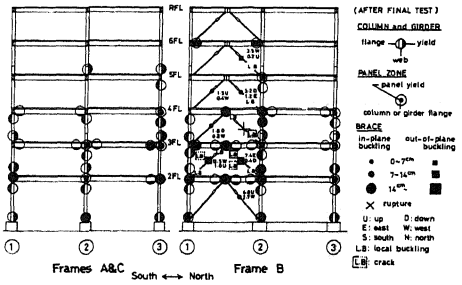

Fig.6 Observed Damage Pattern : Final Test

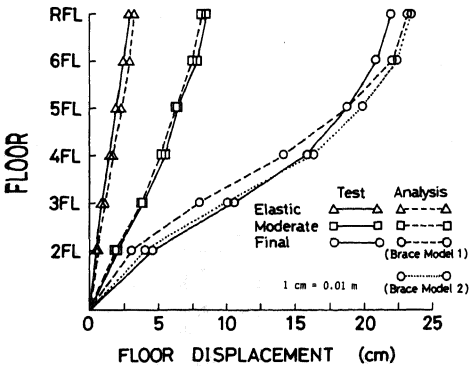

(a) Horizontal Floor Displacements

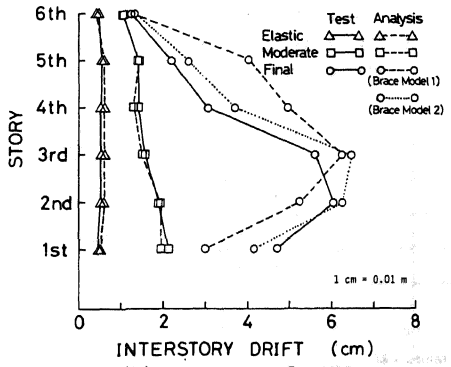

(b) Story Drifts

Fig.7 Envelopes of Maximum Responses

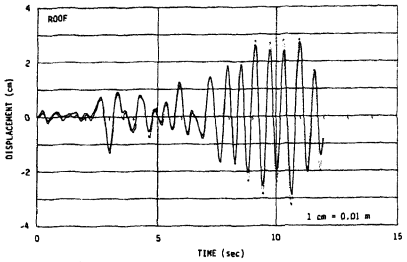

(a) Elastic PSD Test

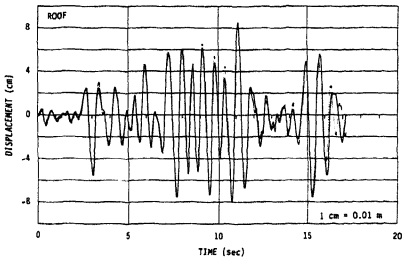

(b) Inelastic PSD Moderate Test

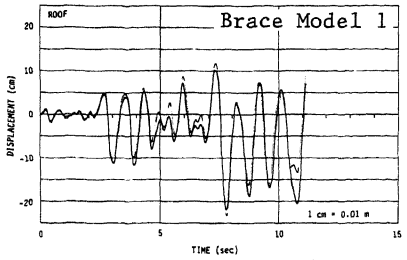

(c) Inelastic PSD Final Test

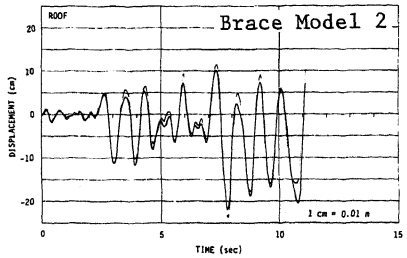

(d) Inelastic PSD Final Test

Fig.8 Horizontal Roof Displacement Time Histories

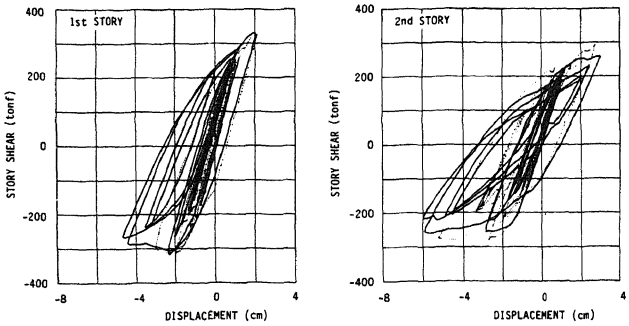

(a) Brace Model 1

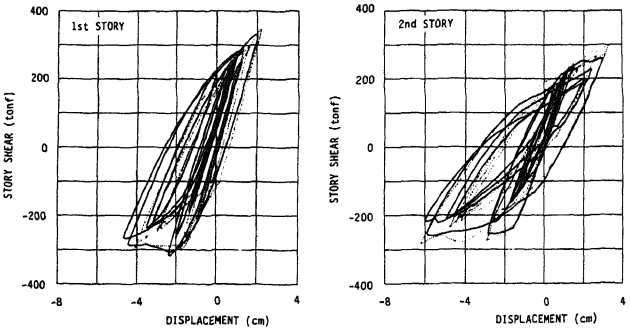

(b) Brace Model 2

Fig.9 Story Shear vs. Story Drift Relationships: Final Test

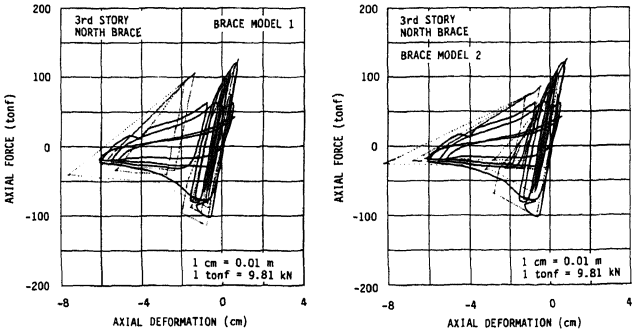

(a) Brace Model 1 (b) Brace Model 2

Fig.10 Axial Force vs. Axial Deformation Relationships

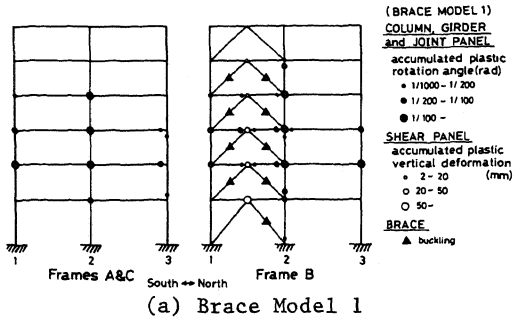

(a) Brace Model 1

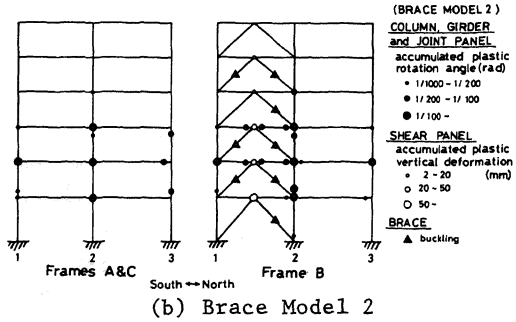

(b) Brace Model 2

Fig.11 Analytical Damage Pattern: Final Test